Reversal of Projected European Summer Precipitation Decline in a Stabilising Climate

A. J. Dittus[1], M. Collins[2], R. Sutton[1], E. Hawkins[1]

[1]National Centre for Atmospheric Science and Department of Meteorology, University of Reading, UK

[2]College of Engineering, Mathematics and Physical Sciences, University of Exeter, Exeter, UK

Corresponding author: Andrea Dittus (a.j.dittus@reading.ac.uk)

Key Points:

- Climate stabilisation experiments show significant differences in projected precipitation compared to high-emission transient scenarios
- Northern European and Mediterranean projected summer drying is partially reversed
- European summer precipitation changes are consistent with the atmospheric response to Atlantic SST changes

Abstract

Precipitation projections in transient climate change scenarios have been extensively studied over multiple climate model generations. Although these simulations have also been used to make projections at specific Global Warming Levels (GWLs), dedicated simulations are more appropriate to study changes in a stabilising climate. Here, we analyse precipitation projections in six multi-century experiments with fixed atmospheric concentrations of greenhouse gases, conducted with the UK Earth System Model (UKESM) and which span a range of GWLs between 1.5 and 5°C of warming. Regions are identified where the sign of precipitation trends in high-emission transient projections is reversed in the stabilisation experiments. For example, stabilisation reverses a summertime precipitation decline across Europe. This precipitation recovery occurs concurrently with changes in the pattern of Atlantic sea surface temperature trends due to a slow recovery of the Atlantic Meridional Overturning Circulation in the stabilisation experiments, along with changes in humidity and atmospheric circulation.

Plain Language Summary

Climate model projections consistently predict that summer precipitation over Europe is expected to decline in the future as global temperatures rise under continued global warming. In our study, we use new climate model simulations that simulate a world where atmospheric concentrations of greenhouse gases are no longer increasing and the rise in global temperatures has slowed down. We show that the summer rainfall decline across Europe can, to some extent, be reversed if global temperatures were to stabilise. This has important implications for adaptation and planning decisions, particularly in so-called climate change 'hot-spots' such as the Mediterranean.

1 Introduction

The 2015 Paris Agreement defines legally binding temperature limits for the 196 signatory parties, with an implied aim to remain below defined temperature thresholds in the long-term. A key question for climate adaptation is understanding what the climate will look like in a net-zero emissions world where global temperatures have roughly stabilised. Many studies have investigated projected climate change at specified Global Warming Levels (GWLs), but a large majority of these projections are extracted from transient simulations with time-varying radiative forcings (e.g. Swaminathan et al. (2022) for projections using the UK Earth System Model; UKESM1). While climate projections under different radiative forcing scenarios have been extensively studied across multiple model generations, there are fewer studies focussing on understanding the regional climate impacts of emission reductions or even cessation.

To date, a few climate model experimental designs to study net-zero climates exist. The Zero Emissions Commitment Model Intercomparison Project (ZECMIP, Jones et al., (2019)) was designed to quantify the amount of committed additional warming following a cessation of CO_2 emissions. By design, this results in a multi-model ensemble stabilising at different GWLs largely depending on the different model climate sensitivities. Other experimental designs have been proposed which focus on sampling specific target GWLs rather than prescribing emission pathways (Sigmond et al., 2020; King, Sniderman, et al., 2021). Fixed concentration experiments, such as the millennial-length simulations contributing to LongRunMIP, have also been used to study climate differences between transient and equilibrated climate states (e.g.

Rugenstein et al., 2019; Callahan et al., 2021; King, Borowiak, et al., 2021). Fixed-concentration experiments such as these continue to warm over time, as the ocean continues to take up heat while atmospheric greenhouse gas (GHG) concentrations remain constant (MacDougall et al., 2020). In contrast, in simulations where GHG emissions, rather than concentrations, are prescribed, atmospheric GHG concentrations decrease over time due to uptake from the ocean and terrestrial carbon sinks, more closely simulating a net-zero climate (MacDougall et al., 2020). While emission-driven experiments are well-suited to study the global mean temperature commitment after reaching net-zero emissions of GHGs, fixed concentration experiments are well-suited to study slow changes in the climate system as it slowly transitions to a new equilibrium state on millennial timescales. Other approaches to investigate temperature stabilisation include using a simple climate model to predict time-varying concentration pathways consistent with stabilisation at global warming level targets (Sanderson et al., 2017) or the recently developed adaptive emission reduction approach (AERA, Terhaar et al., 2022).

In this paper, we seek to investigate how regional climates are not uniquely determined by their associated GWL. We explore how the rate of climate change is an important factor in shaping regional patterns of climate change. To do this, we exploit an ensemble of six multi-centennial simulations conducted under fixed atmospheric concentrations of GHGs with UKESM1, specifically designed to span a range of GWLs between 1.5 and 5°C above pre-industrial by branching-off from ScenarioMIP simulations (O'Neill et al., 2016) at different times. Despite the slow residual warming, the experiments used are referred to as stabilisation experiments hereafter for simplicity. We identify regions where precipitation projections at different global warming levels (GWLs) in the stabilisation experiments differ in sign from their rapidly warming transient counterparts, focussing on Europe in particular.

2 Climate model ensemble design

Six 500-year long climate model simulations were performed with the UKESM1-0-LL Earth System Model under constant external forcing conditions.This model has an atmospheric resolution of 1.25°×1.875° on 85 vertical levels and a 1° ocean, and includes the following earth system components: a terrestrial carbon and nitrogen cycle; ocean biogeochemistry (BGC) and a unified troposphere-stratosphere chemistry model, tightly coupled to a multi-species modal aerosol scheme (Sellar et al., 2019). The terrestrial biogeochemistry includes dynamic vegetation and a representation of agricultural land use change. Its climate sensitivity is 5.4K (Sellar et al., 2019). The simulations were designed to target a range of global warming levels to explore projected climate change between 1.5 and 5°C above pre-industrial levels in a fully coupled, state-of-art Earth System Model (ESM). The external forcings for each simulation are held at the level they were at in a parent ScenarioMIP simulation at the time the simulations are branched off. In the case of GHGs, that corresponds to constant concentrations and for anthropogenic aerosols it corresponds to constant emissions. The vegetation is dynamic, but each grid cell has a prescribed crop and pasture fraction based on the conditions of their parent simulations at the point of branching-off. Solar and volcanic forcing are set to the forcings used in the pre-industrial control simulations. The six experiments are branched from the historical and ScenarioMIP experiments as follows:

- 2014 in historical
- 2020 in SSP3-7.0
- 2025 in SSP3-7.0
- 2025 in SSP2-4.5
- 2030 in SSP1-1.9
- 2040 in SSP3-7.0

All simulations are branched from the first initial condition realisation of the parent ScenarioMIP experiment (r1i1p1f2 in CMIP6 nomenclature). The importance of branching from different scenarios and therefore having differences in the spatial pattern of anthropogenic aerosols and land-use change will be assessed in separate work. The results presented in this paper are not sensitive to the parent scenario the simulations were branched from.

The climate response in the six fixed concentration experiments (500 years each) is compared to the UKESM1-0-LL CMIP6 ScenarioMIP SSP3-7.0 experiments (86 years each), of which there are 16 initial condition members. Mitigation scenarios are not considered in this study due to fewer (5) ensemble members being available for this model and to avoid conflating responses due to other factors such as rapid changes in aerosols in scenarios like SSP1-1.9, in contrast to relatively stable aerosol emissions in SSP3-7.0 (Wilcox et al., 2020).

3 Results

3.1 Global overview of simulated climate characteristics

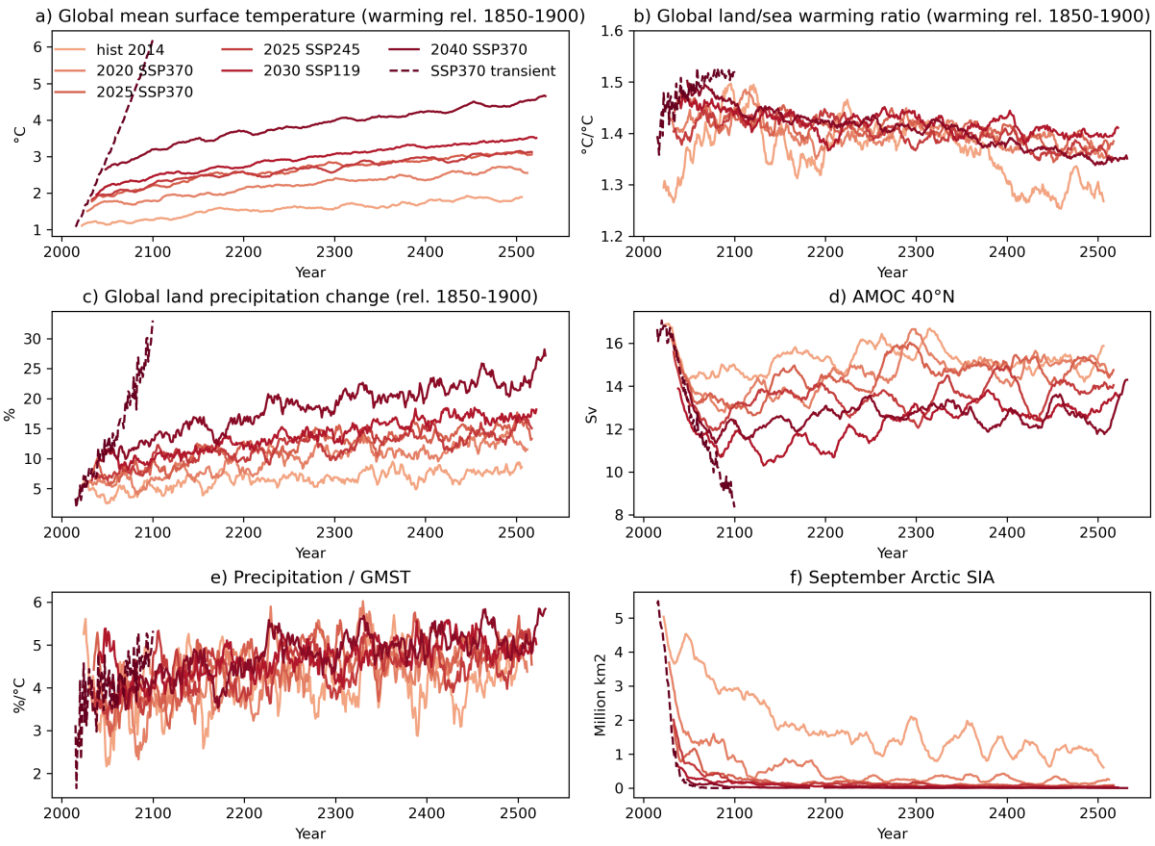

Figure 1. 16-year running means of global mean surface temperature (a), the land-sea warming ratio (b), global land precipitation (c), the AMOC at 40°N (d), hydrological sensitivity defined as global land precipitation divided by GMST (e), and September Arctic sea-ice area (f) in the various simulations. The reference time period for anomalies (panels a, b and c) is 1850-1900. The SSP3-7.0 transient projections are a 16-member ensemble mean and are not temporally smoothed.

As expected for this experimental setup, the fixed concentration experiments show ongoing global warming over the multi-centennial length of the experiments (Figure 1a; solid lines). However, the climate warms at a much slower rate in the fixed concentration simulations than the SSP3-7.0 scenario (dashed purple line). In the fixed concentration experiments, the top-of-atmosphere (TOA) radiation imbalance is declining but remains positive even after 500 years, explaining the continuing slow warming in these simulations (Figure S2). The amplitude and timescales of the reduction in TOA radiation imbalance in our fixed concentration experiments is consistent with results from LongRunMIP (Rugenstein et al., 2019). We can therefore use the fixed concentration experiments to investigate how a stabilising climate differs from a rapidly warming one. Existing studies have shown differences in the warming pattern for the same global warming levels between transient and stabilisation experiments (e.g. King, Borowiak, et al., 2021), with relatively reduced warming over land and enhanced warming over the oceans in the stabilisation experiments relative to the typical transient experiments. A similar pattern is also found in our experiments (Figure S1), resulting in a slowly declining land/sea warming ratio in the stabilisation experiments (Figure 1b). This slow decline in the land/sea warming ratio is in contrast to the increase in the land/sea warming ratio seen in SSP3-7.0, reflecting a strong amplification of the warming over land.

Stabilisation is also expected to change sea-surface temperature patterns and affect ocean circulation. The Atlantic Meridional Overturning Circulation (AMOC) is shown for approximately 40°N as obtained from the Overturning Mass Streamfunction (CMIP6 variable 'msftyz'). The maximum value across all depth ranges is used (i.e. the depth corresponding to the streamfunction maximum is time-varying). In transient experiments such as SSP3-7.0, the AMOC rapidly declines, consistent with previous studies (Figure 1d and e.g. Weijer et al., 2020). In the stabilisation experiments, the AMOC initially declines for several decades, but eventually begins to recover and subsequently increases under constant forcing conditions (Figure 1d). This is comparable to findings from Sigmond et al. (2020), who found an AMOC recovery in their emission-driven GWL experiments, but contrasts with the persistent weakening of the AMOC in the overshoot experiments of Delworth et al. (2022), where global temperatures peak in the 2050s and decline thereafter. In our fixed concentration experiments, September Arctic sea-ice rapidly declines, approaching ice-free conditions within the first 100 years for the warmer experiments. The AMOC recovery could be tied to timescales of when Arctic sea-ice loss stabilises (Nobre et al. 2023) but we do not investigate the mechanisms driving the AMOC recovery further here.

Globally averaged land precipitation is increasing in both the transient and the stabilisation experiments, but at different rates, approximately following the different rates of global warming (Figure 1c). The global land hydrological sensitivity spans a comparable range for both the transient and fixed concentration experiments, but both vary in time (Figure 1e). However, regional-scale precipitation projections over land are more complicated due to the importance of different mechanisms, including atmospheric circulation changes and land-surface feedbacks (e.g. Byrne & O'Gorman, 2015; Seager et al., 2014). In the following section, we analyse regional-scale precipitation projections in the transient and stabilisation experiments for the 46 land regions used in the IPCC 6th Assessment Report (Iturbide et al., 2020). All regionally averaged results are presented for data that has been masked to include land points only (Figures 2 and 3).

3.2 Global and seasonal precipitation projections

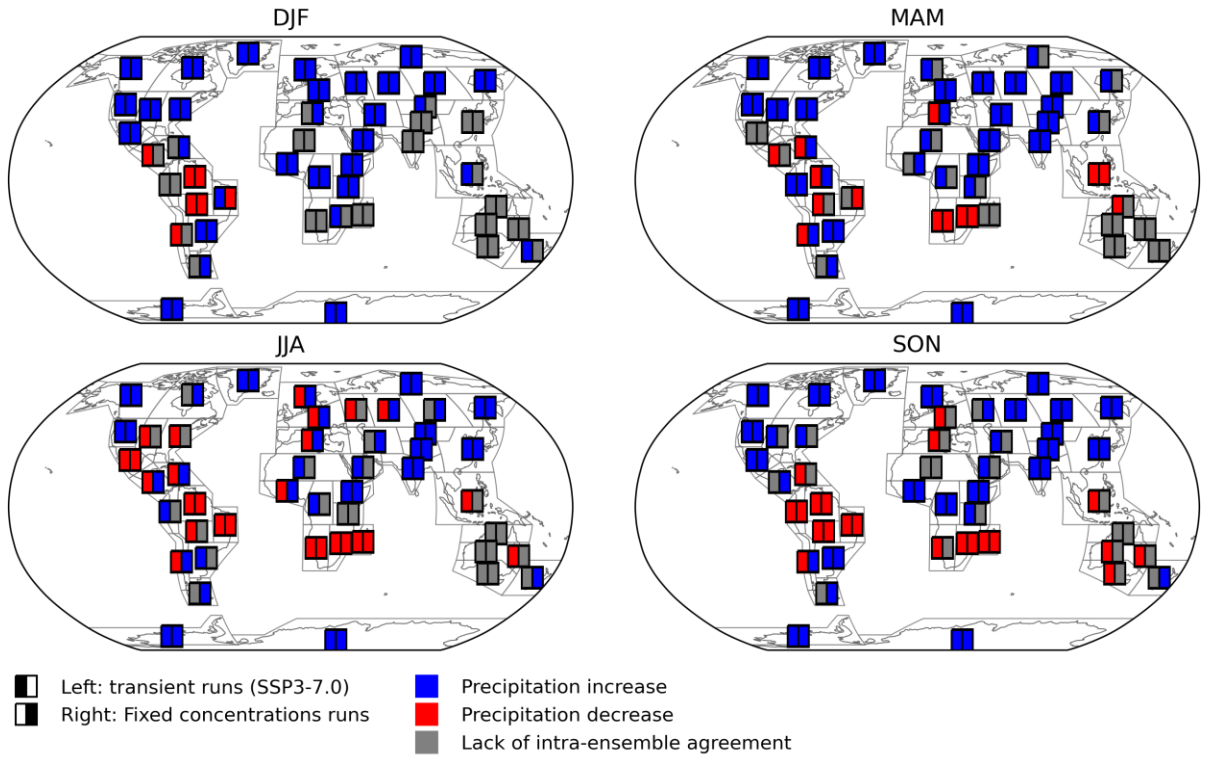

Figure 2 Overview of precipitation trends in SSP3-7.0 (left rectangle) and the fixed concentration experiments (right rectangle) in all seasons for different land regions. Blue indicates a positive precipitation trend and red is used used for negative precipitation trends. These colours are shown where > 80% of ensemble members agree on the sign of the trend. Grey rectangles are used where < 80% of ensemble members agree on sign, and therefore represents lack of agreement across the ensemble. The trends are calculated over the full duration of the simulations (86 and 500 years respectively).

When considering the regional differences between transient and stabilisation simulations it is clear that precipitation trends show some striking differences. Figure 2 summarises projected precipitation trends in all IPCC AR6 land regions for each season (Iturbide et al., 2020). The colours in Figure 2 indicate the sign of the trends in each region for the transient experiments (left rectangle), and the fixed concentration runs (right rectangle): blue for increasing trends, red for decreasing trends, and grey for lack of agreement across ensemble members. For boreal summer (JJA) there is a striking feature across Europe where summer drying in the transient simulations becomes wettening in the stablisation simulations; note this is purely a summer phenomenon, as precipitation increases in the transient simulations in the other seasons of the year. The Mediterranean trend reversal occurs in both MAM and JJA, with a precipitation increase also seen in DJF in the fixed concentration experiments. No agreement on the sign of the trend across ensemble members in the fixed concentration experiments in SON indicates a possible stabilisation. We consider these European changes further below, noting that UKESM1-0 achieved a ‘satisfactory’ performance classification for precipitation in all European regions (Palmer et al. 2023).

Elsewhere, a reversal of a transient precipitation decline occurs in many regions across the globe: the Carribean in MAM & JJA; North-East (DJF), Northern (MAM), South-West (all seasons except DJF) South America; Western Africa in JJA. A possible stabilisation (grey) of a transient

precipitation decline also occurs in several other Central and South American regions, Eastern North America (JJA), Australia (MAM, JJA and SON) and Western Southern-Africa (SON).

Overall, reversals of drying trends occur in multiple regions and seasons, while there are no robust reversals of wettening trends, although changes from a wettening trend to a stabilisation (grey) do occur in some instances. However, we do not investigate these instances further here. The sensitivity to the time period over which the trends are calculated is illustrated in Figures S4 and S5.

3.3 European summer precipitation projections and associated patterns of change

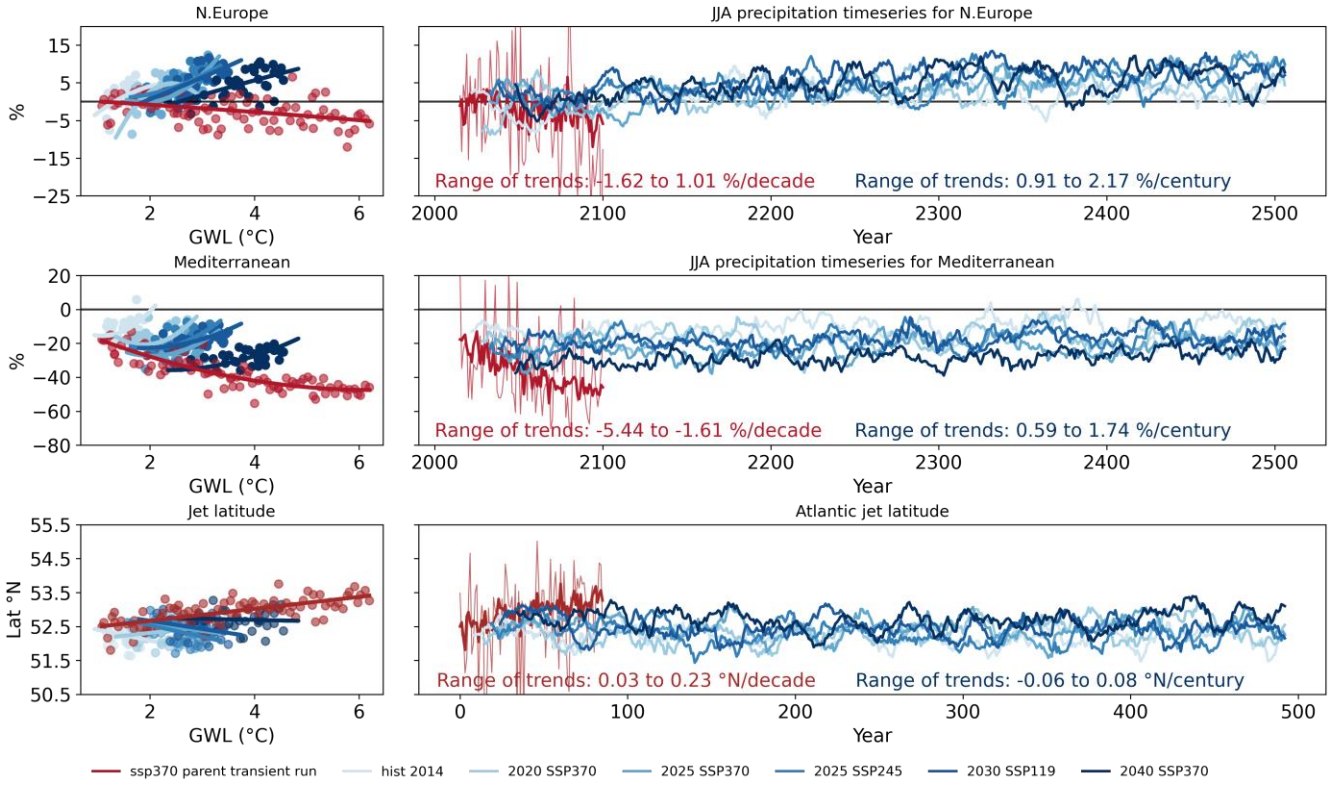

Figure 3 JJA precipitation projections in SSP3-7.0 (red) and the stabilisation experiments (blues) for a) Northern Europe and b) the Mediterranean. Panel c) shows the summer Atlantic jet latitude following the definition of Ceppi et al. (2018). The left panels show the projected changes as a function of GWLs, and the right panels as a function of time. All stabilisation experiments are smoothed by a 16-year running mean, while the transient experiments are a 16-member ensemble average. A single SSP3-7.0 simulation is also shown (thin brown line), representing the parent simulation for those stabilisation experiments that are branched from SSP3-7.0. Only every 16th point is shown on the scatterplot for illustration purposes, but the regression in the left panel is performed over all data points. A quadratic least squares fit was performed for the precipitation data and a linear fit was used for the jet latitude index (left panels).

In boreal summer, transient climate projections have long shown a robust decrease in precipitation over the Mediterranean region (e.g. Giorgi & Lionello, 2008) and the region is considered a climate change 'hot-spot' (Giorgi, 2006). Northern European projections are more uncertain due to different model responses in atmospheric circulation changes but also tend to

project a precipitation decline (e.g. Brunner et al., 2019). The UKESM1 SSP3-7.0 transient projections are in agreement with this finding (Figure 3; red). In the Mediterranean, the projected precipitation decline under SSP3-7.0 is approximately -48% by the end of the century relative to 1850-1900, compared to -7% for Northern Europe (Figure 3). However, regardless of which scenario and year the fixed concentration experiments were branched from, *the stabilisation experiments show a wettening trend instead of a drying, reversing the precipitation decline seen in the transient projections*. This is particularly striking when precipitation change is viewed as a function of global mean warming (Figure 3, left): in the transient projections, precipitation decreases approximately linearly with additional warming. In contrast, in the stabilisation experiments, precipitation increases with further warming within a single simulation. Across multiple simulations, the warming level does not uniquely define a precipitation level, suggesting that the timescale since branching-off from the parent scenario simulation is an important control on the projected precipitation amplitude. We note that for this model in SSP1-1.9 there is also a reversal in the Mediterranean drying trend as global temperatures cool after 2050 although we do not consider those experiments further here.

By the end of the stabilisation simulations, Mediterranean precipitation is still below the 1850-1900 baseline. In contrast, Northern Europe precipitation overshoots the reference baseline by the 2nd century of the simulations. Expressed as a percentage change relative to 1850-1900, the precipitation deficit is much larger in the Mediterranean than in Northern Europe. Perhaps unsurprisingly, internal variability is larger in the Northern Europe region, with a separation between the six stabilisation runs not clearly discernible by eye. In contrast, in the Mediterranean, the separation between the different stabilisation experiments is clear: the lowest warming runs, starting off with a smaller precipitation deficit, consistently have a smaller precipitation deficit than the higher warming simulations. This clear separation between the different simulations in the Mediterranean persisting to the end of the 500-year simulations implies that while the precipitation deficit might be partially reversible over long timescales, the recovery timescale is so long that the initial deficit still matters centuries later.

The mechanisms explaining this reversal of summertime drying across Europe warrant some discussion. To compare trend patterns between the transient and stabilisation experiments, Figure 4 shows the linear regression patterns in the variable of interest divided by the trend in global average surface temperature. This ensures that the scaled patterns are of comparable magnitude between both sets of experiments. It also ensures that the patterns can be averaged across the different stabilisation simulations. It is however important to note here that the magnitude of the absolute trends is substantially larger in the transient simulations than the stabilisation experiments (see Figure 1). As a measure of robustness of the trends, lack of stippling indicates that > 80% of available ensemble members per experiment agree on the sign of the trend.

The pattern of warming across the North Atlantic differs substantially between the transient and stabilisation experiments (Figure 4; top row). The strong warming in the subpolar gyre region in the stabilisation experiments is consistent with a strengthened northward heat transport due to a partial recovery in the AMOC (Figure S3), in contrast to the AMOC decline in the transient experiments (Figure 1d). While the jet is shifting polewards in the transient runs, the jet latitude in the stabilisation experiments is roughly stabilised at the level of branching-off from the parent transient run, with perhaps an indication of a weak equatorward trend in some of the runs (Figure

3). This is potentially consistent with a reduced meridional temperature gradient induced by the subpolar gyre warming.

The specific humidity changes in the fixed concentration experiments over the North Atlantic closely mirror the pattern of warming, with increased specific humidity in the fixed concentration runs in the subpolar gyre and along the eastern coast of the North Atlantic. Relative humidity and precipitable water content in the stabilisation experiments also increase (not shown). These results suggest that concurrent humidity changes are an important factor explaining the precipitation increases in the stabilisation runs. There are also indications that changing SST patterns could lead to atmospheric circulation changes in the North Atlantic. A low-pressure anomaly southwest of the UK and Ireland and changes in the zonal wind speed consistent with a southward shift of the jet are both robust across ensemble members in the JJA mean. These atmospheric circulation changes could contribute to the positive precipitation trends in Northern Europe, but their exact role is difficult to quantify. We further note that the strongest surface circulation changes are found for MAM (see Figure S6) which also shows a precipitation reversal in the Mediterranean region and so precursor wetter conditions may also play a role for the reversed trends in summer (e.g. Leutwyler et al., 2021).

Summer precipitation in Europe mostly occurs in transient weather systems, including intense convective events. The moisture source for this rainfall either comes from storms as they pass over the ocean or is evaporated from the land surface. Without a detailed analysis of moisture sources, and dynamical and thermodynamical components of precipitation (e.g. Chadwick et al., 2016), it is not possible to quantitatively attribute changes in the different experiments to specific physical processes. Nevertheless, this would be a suitable subject for future research, particularly in the context of understanding projected changes in mean and extreme precipitation events.

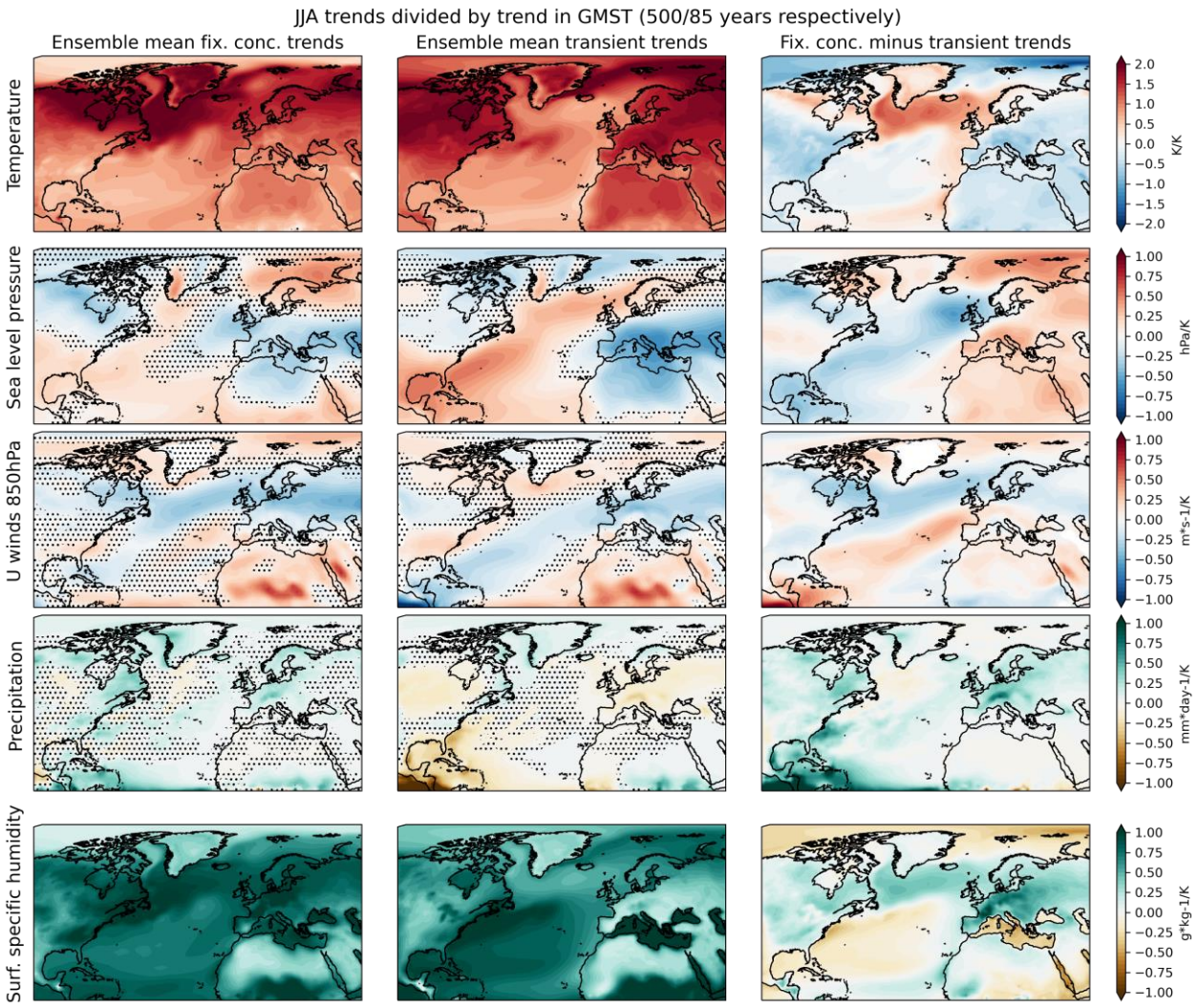

Figure 4 JJA trends in air temperatures, sea level pressures, 850 hPa zonal winds, precipitation and surface specific humidity in the 6-member ensemble mean of the fixed concentration runs (left) and the transient SSP-3-7.0 16-member ensemble mean (middle). The trends were computed over the full timeperiod, 86 and 500 years respectively. The difference in the trend patterns between fixed concentrations minus transient runs is shown on the right. All trend patterns have been scaled (i.e., divided by) the trend in global mean surface temperatures, ensuring that the patterns across all simulations are comparable. Unscaled, the transient trends are much larger in magnitude than the trends in the fixed concentration experiments. Lack of stippling indicates that >80% of ensemble members agree on the sign of the trend (at least 5/6 in the left column, and 13/16 in the middle column).

4 Discussion and conclusions

The projected summertime (JJA) precipitation decline across different European regions in transient scenarios is well studied (e.g. Tuel & Eltahir, 2021). Studies have shown that the assumption of a linear relationship between projected local precipitation change and increasing GWLs is well justified in most cases for transient climate change simulations and observations (e.g. Seneviratne & Hauser, 2020). Our results show that this relationship holds in the UKESM1 transient projections (brown dots and lines, Figure 3) but this assumption no longer applies in the fixed concentration simulations we have used to study climate stabilisation (blue dots and lines;

Figure 3). Other stabilisation experimental designs have also identified instances where precipitation recovers from a decline in rapidly-warming transient projections in both hemispheres (e.g. Sniderman et al., 2019; Grose & King, 2023 for the Southern Hemisphere). For Europe, Delworth et al. (2022) found a recovery of summertime precipitation in the Mediterranean, and identified a dependence of the winter precipitation trends in the Mediterranean upon the state of the AMOC in their simulations. Globally, Zappa et al. (2020) identified three Mediterranean-like regions where the time evolution of the local hydro-climate response did not scale linearly with global mean warming under stabilisation scenarios. They linked these deviations from a simple pattern scaling to different timescales of the response: rapid adjustments, fast changes in sea-surface temperature patterns and slow changes in sea-surface temperature patterns. Our results are consistent with this perspective, in that slow changes in sea surface temperature play a key role in changing the characteristics of regional precipitation in Europe. Our results also highlight further that the regional climates are not uniquely determined by GWL but also depend on the regional pattern of warming over the Atlantic associated with slow changes in the ocean circulation. For the Mediterranean, the rates of recovery in precipitation are comparable across the different ensemble members, which implies that the point at which concentrations are fixed (i.e. the beginning of 'stabilisation') is an important factor that could have impacts on precipitation levels even centuries later.

The results presented here and elsewhere highlight an important finding that *in many regions and seasons, a precipitation decline under transient warming may be reversible to some extent, if global temperatures stabilise*. The consistency of our Mediterranean results with previous studies suggests that these findings are likely to be robust across different climate models. For Northern Europe, we identify a precipitation increase in summer in the stabilisation experiments, overshooting the pre-industrial baseline by the 2nd century of the simulations. Atmospheric circulation changes associated with a change in the surface temperature pattern over the North Atlantic, consistent with a slow recovery of the AMOC, are also found. Future studies with other models or different experimental designs will help quantify the sensitivity of the Atlantic circulation changes and northern European wettening to model structural uncertainty and experimental design choices. The precipitation response in mitigation scenarios where future temperature increases are limited also warrant further investigation.

In summary, our results show that climate projections under stabilised warming can substantially deviate from expectations derived from transient climate change projections. Reversals in the sign of precipitation projections would have important implications for adaptation and planning decisions. In particular, the prospect of halting an ongoing precipitation decline would have important implications for water resources management in so-called climate change 'hotspots' such as the Mediterranean. More research is needed to understand how these differences affect changes in the frequency and intensity of extreme precipitation events in a stabilised world.

Acknowledgments

The authors would like to thank Dr. Alistair Sellar from the UK Met Office for his help in generating the time slice ancillaries required to run the experiments described in this paper. We also thank Dr. David Sexton for discussions on the experimental design and preliminary analysis of the runs. We thank Dr. Ben Harvey and Dr. William Ingram for useful discussions on an early presentation of the work. We acknowledge use of the Monsoon2 system, a collaborative facility

supplied under the Joint Weather and Climate Research Programme, a strategic partnership between the Met Office and the Natural Environment Research Council.

Open Research

The code required to reproduce the figures in this paper is available in a public GitHub repository here: https://github.com/andreadittus/EuropeanPrecipitation_paper. The UKESM1 stabilisation model data required to reproduce the work in this publication are available here for the purposes of review: https://gws-access.jasmin.ac.uk/public/smurphs/REAL_precip_paper/, and will be available in the CEDA archive by the publication date (deposit in progress).

References

Brunner, L., Lorenz, R., Zumwald, M., & Knutti, R. (2019). Quantifying uncertainty in European climate projections using combined performance-independence weighting. *Environmental Research Letters*, *14*(12), 124010. https://doi.org/10.1088/1748-9326/ab492f

Byrne, M. P., & O'Gorman, P. A. (2015). The Response of Precipitation Minus Evapotranspiration to Climate Warming: Why the "Wet-Get-Wetter, Dry-Get-Drier" Scaling Does Not Hold over Land*. *Journal of Climate*, *28*(20), 8078–8092. https://doi.org/10.1175/JCLI-D-15-0369.1

Callahan, C. W., Chen, C., Rugenstein, M., Bloch-Johnson, J., Yang, S., & Moyer, E. J. (2021). Robust decrease in El Niño/Southern Oscillation amplitude under long-term warming. *Nature Climate Change*, *11*(9), 752–757. https://doi.org/10.1038/s41558-021-01099-2

Ceppi, P., Zappa, G., Shepherd, T. G., & Gregory, J. M. (2018). Fast and Slow Components of the Extratropical Atmospheric Circulation Response to CO2 Forcing. *Journal of Climate*, *31*(3), 1091–1105. https://doi.org/10.1175/JCLI-D-17-0323.1

Chadwick, R., Good, P., & Willett, K. (2016). A Simple Moisture Advection Model of Specific Humidity Change over Land in Response to SST Warming. *Journal of Climate*, *29*(21), 7613–7632. https://doi.org/10.1175/JCLI-D-16-0241.1

Delworth, T. L., Cooke, W. F., Naik, V., Paynter, D., & Zhang, L. (2022). A weakened AMOC may prolong greenhouse gas–induced Mediterranean drying even with significant and rapid climate change mitigation. *Proceedings of the National Academy of Sciences*, *119*(35), e2116655119. https://doi.org/10.1073/pnas.2116655119

Giorgi, F. (2006). Climate change hot-spots. *Geophysical Research Letters*, *33*(8), L08707. https://doi.org/10.1029/2006GL025734

Giorgi, Filippo, & Lionello, P. (2008). Climate change projections for the Mediterranean region. *Global and Planetary Change*, *63*(2–3), 90–104. https://doi.org/10.1016/j.gloplacha.2007.09.005

Grose, M. R., & King, A. D. (2023). The circulation and rainfall response in the southern hemisphere extra-tropics to climate stabilisation. *Weather and Climate Extremes*, *41*, 100577. https://doi.org/10.1016/j.wace.2023.100577

Iturbide, M., Gutiérrez, J. M., Alves, L. M., Bedia, J., Cerezo-Mota, R., Cimadevilla, E., et al. (2020). An update of IPCC climate reference regions for subcontinental analysis of climate model data: definition and aggregated datasets. *Earth System Science Data*, *12*(4), 2959–2970. https://doi.org/10.5194/essd-12-2959-2020

Jones, C. D., Frölicher, T. L., Koven, C., MacDougall, A. H., Matthews, H. D., Zickfeld, K., et al. (2019). The Zero Emissions Commitment Model Intercomparison Project (ZECMIP) contribution to C4MIP: quantifying committed climate changes following zero carbon emissions. *Geoscientific Model Development*, *12*(10), 4375–4385. https://doi.org/10.5194/gmd-12-4375-2019

King, A. D., Sniderman, J. M. K., Dittus, A. J., Brown, J. R., Hawkins, E., & Ziehn, T. (2021). Studying climate stabilization at Paris Agreement levels. *Nature Climate Change*, *11*(12), 1010–1013. https://doi.org/10.1038/s41558-021-01225-0

King, A. D., Borowiak, A. R., Brown, J. R., Frame, D. J., Harrington, L. J., Min, S., et al. (2021). Transient and Quasi-Equilibrium Climate States at 1.5°C and 2°C Global Warming. *Earth's Future*, *9*(11). https://doi.org/10.1029/2021EF002274

406 Leutwyler, D., Imamovic, A., & Schär, C. (2021). The Continental-Scale Soil-Moisture Precipitation Feedback in
407 Europe with Parameterized and Explicit Convection. *Journal of Climate*, 1–56. https://doi.org/10.1175/JCLI-D-20-
408 0415.1
409 MacDougall, A. H., Frölicher, T. L., Jones, C. D., Rogelj, J., Matthews, H. D., Zickfeld, K., et al. (2020). Is there
410 warming in the pipeline? A multi-model analysis of the Zero Emissions Commitment from CO2. *Biogeosciences*,
411 *17*, 2987–3016. https://doi.org/10.5194/bg-17-2987-2020
412 Nobre, P., Veiga, S. F., Giarolla, E., Marquez, A. L., Da Silva, M. B., Capistrano, V. B., et al. (2023). AMOC
413 decline and recovery in a warmer climate. *Scientific Reports*, *13*(1), 15928. https://doi.org/10.1038/s41598-023-
414 43143-5
415 O'Neill, B. C., Tebaldi, C., van Vuuren, D. P., Eyring, V., Friedlingstein, P., Hurtt, G., et al. (2016). The Scenario
416 Model Intercomparison Project (ScenarioMIP) for CMIP6. *Geoscientific Model Development*, *9*(9), 3461–3482.
417 https://doi.org/10.5194/gmd-9-3461-2016
418 Palmer, T. E., McSweeney, C. F., Booth, B. B. B., Priestley, M. D. K., Davini, P., Brunner, L., et al. (2023).
419 Performance-based sub-selection of CMIP6 models for impact assessments in Europe. *Earth System Dynamics*,
420 *14*(2), 457–483. https://doi.org/10.5194/esd-14-457-2023
421 Rugenstein, M., Bloch-Johnson, J., Abe-Ouchi, A., Andrews, T., Beyerle, U., Cao, L., et al. (2019). LongRunMIP:
422 Motivation and Design for a Large Collection of Millennial-Length AOGCM Simulations. *Bulletin of the American*
423 *Meteorological Society*, *100*(12), 2551–2570. https://doi.org/10.1175/BAMS-D-19-0068.1
424 Sanderson, B. M., Xu, Y., Tebaldi, C., Wehner, M., O'Neill, B., Jahn, A., et al. (2017). Community climate
425 simulations to assess avoided impacts in 1.5 and 2 °C futures. *Earth System Dynamics*, *8*(3), 827–847.
426 https://doi.org/10.5194/esd-8-827-2017
427 Seager, R., Liu, H., Henderson, N., Simpson, I., Kelley, C., Shaw, T., et al. (2014). Causes of Increasing
428 Aridification of the Mediterranean Region in Response to Rising Greenhouse Gases*. *Journal of Climate*, *27*(12),
429 4655–4676. https://doi.org/10.1175/JCLI-D-13-00446.1
430 Sellar, A. A., Jones, C. G., Mulcahy, J. P., Tang, Y., Yool, A., Wiltshire, A., et al. (2019). UKESM1: Description
431 and Evaluation of the U.K. Earth System Model. *Journal of Advances in Modeling Earth Systems*, *11*(12), 4513–
432 4558. https://doi.org/10.1029/2019MS001739
433 Seneviratne, S. I., & Hauser, M. (2020). Regional Climate Sensitivity of Climate Extremes in CMIP6 Versus
434 CMIP5 Multimodel Ensembles. *Earth's Future*, *8*(9). https://doi.org/10.1029/2019EF001474
435 Sigmond, M., Fyfe, J. C., Saenko, O. A., & Swart, N. C. (2020). Ongoing AMOC and related sea-level and
436 temperature changes after achieving the Paris targets. *Nature Climate Change*, *10*(7), 672–677.
437 https://doi.org/10.1038/s41558-020-0786-0
438 Sniderman, J. M. K., Brown, J. R., Woodhead, J. D., King, A. D., Gillett, N. P., Tokarska, K. B., et al. (2019).
439 Southern Hemisphere subtropical drying as a transient response to warming. *Nature Climate Change*, *9*(3), 232–236.
440 https://doi.org/10.1038/s41558-019-0397-9
441 Swaminathan, R., Parker, R. J., Jones, C. G., Allan, R. P., Quaife, T., Kelley, D. I., et al. (2022). The Physical
442 Climate at Global Warming Thresholds as Seen in the U.K. Earth System Model. *Journal of Climate*, *35*(1), 29–48.
443 https://doi.org/10.1175/JCLI-D-21-0234.1
444 Terhaar, J., Frölicher, T. L., Aschwanden, M. T., Friedlingstein, P., & Joos, F. (2022). Adaptive emission reduction
445 approach to reach any global warming target. *Nature Climate Change*, *12*(12), 1136–1142.
446 https://doi.org/10.1038/s41558-022-01537-9
447 Tuel, A., & Eltahir, E. A. B. (2021). Mechanisms of European summer drying under climate change. *Journal of*
448 *Climate*, 1–51. https://doi.org/10.1175/JCLI-D-20-0968.1
449 Weijer, W., Cheng, W., Garuba, O. A., Hu, A., & Nadiga, B. T. (2020). CMIP6 Models Predict Significant 21st
450 Century Decline of the Atlantic Meridional Overturning Circulation. *Geophysical Research Letters*, *47*(12).
451 https://doi.org/10.1029/2019GL086075
452 Wilcox, L. J., Liu, Z., Samset, B. H., Hawkins, E., Lund, M. T., Nordling, K., et al. (2020). Accelerated increases in
453 global and Asian summer monsoon precipitation from future aerosol reductions. *Atmospheric Chemistry and*
454 *Physics*, *20*(20), 11955–11977. https://doi.org/10.5194/acp-20-11955-2020
455 Zappa, G., Ceppi, P., & Shepherd, T. G. (2020). Time-evolving sea-surface warming patterns modulate the climate
456 change response of subtropical precipitation over land. *Proceedings of the National Academy of Sciences*, *117*(9),
457 4539–4545. https://doi.org/10.1073/pnas.1911015117
458
459

460

Figure 2.

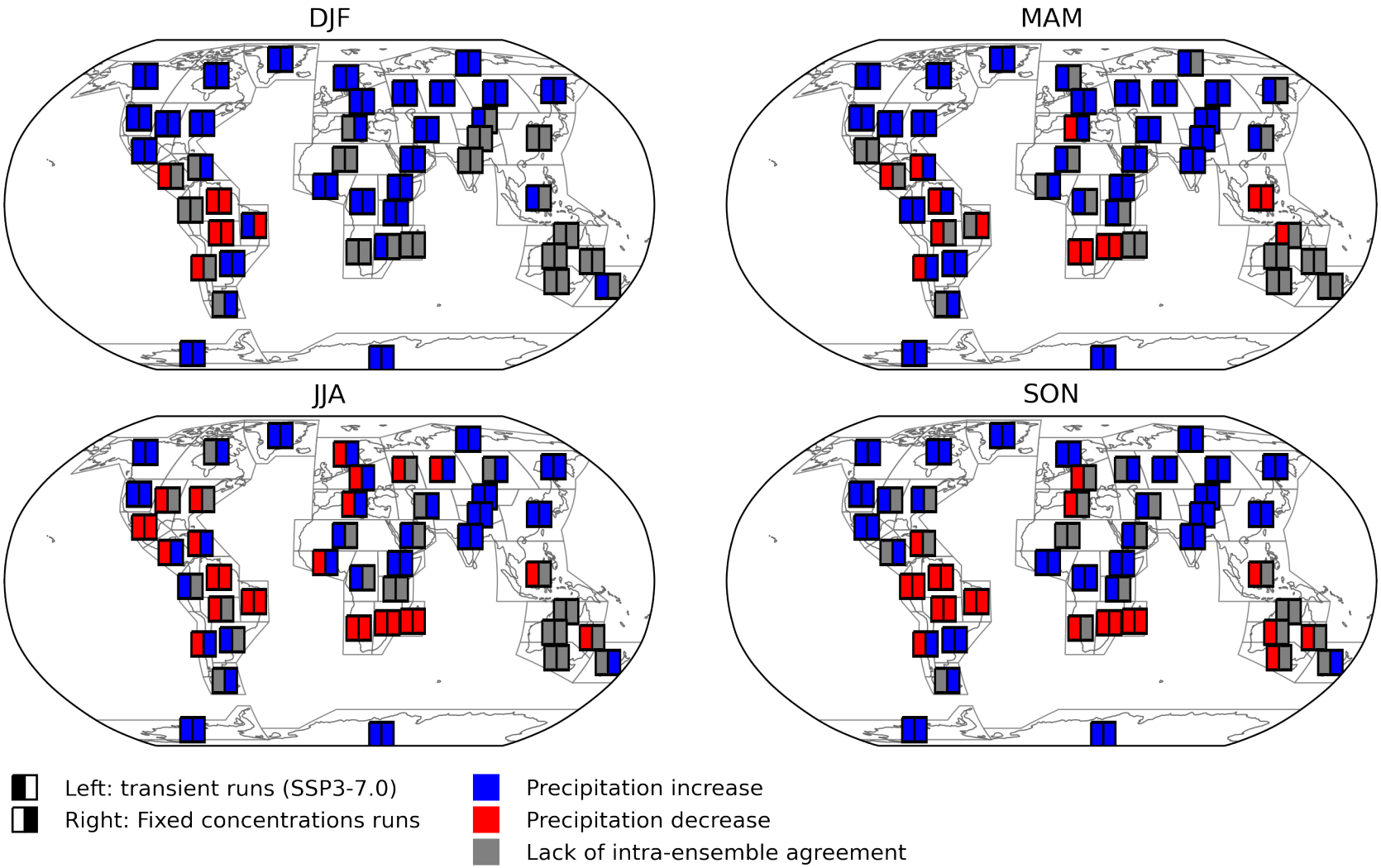
DJF
MAM
JJA
SON
Left: transient runs (SSP3-7.0)
Right: Fixed concentrations runs
Precipitation increase
Precipitation decrease
Lack of intra-ensemble agreement

Figure 1.

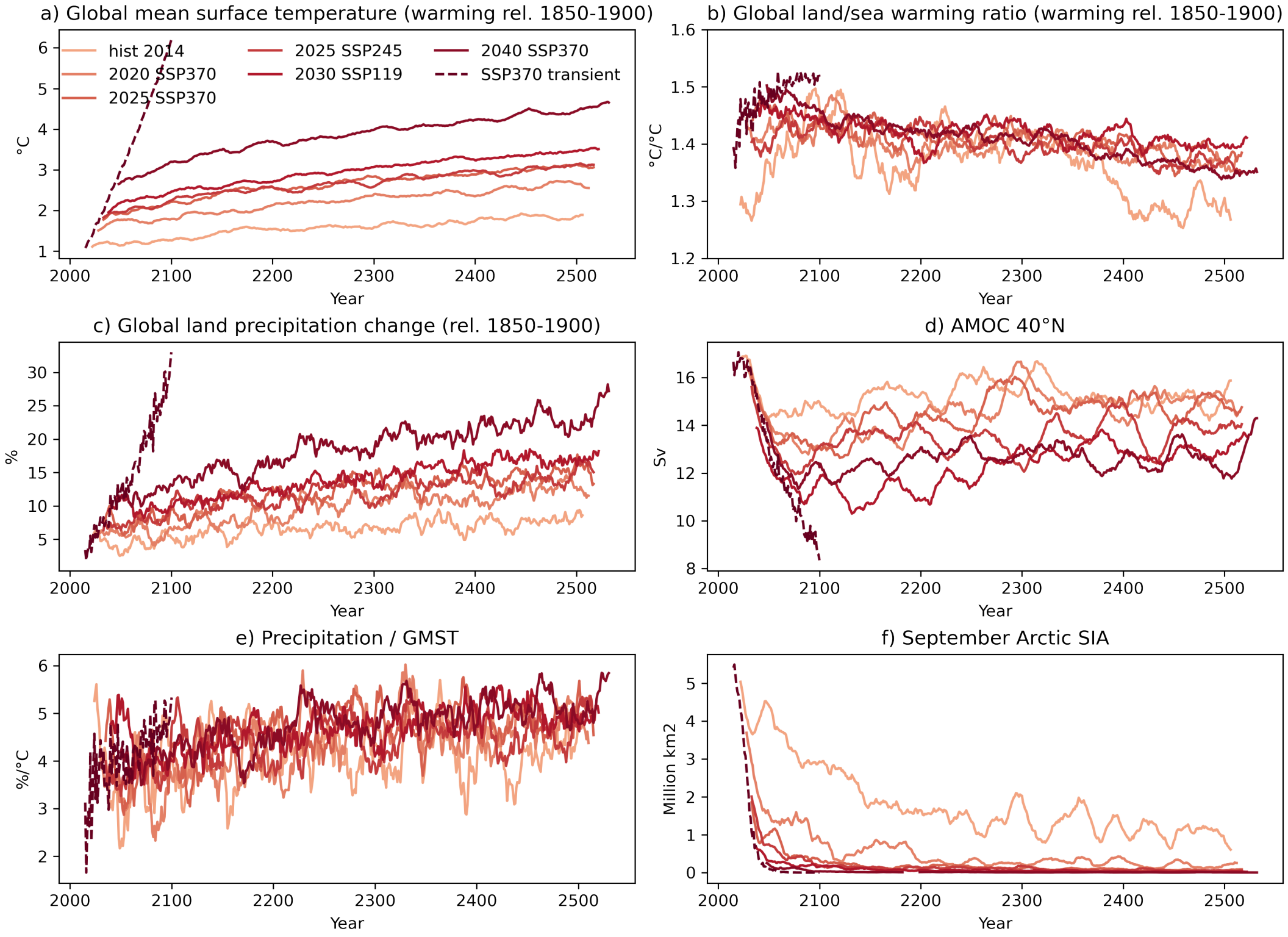
a) Global mean surface temperature (warming rel. 1850-1900)
hist 2014
2020 SSP370
2025 SSP370
2025 SSP245
2030 SSP119
2040 SSP370
SSP370 transient
°C
Year
b) Global land/sea warming ratio (warming rel. 1850-1900)
°C/°C
Year
c) Global land precipitation change (rel. 1850-1900)
%
Year
d) AMOC 40°N
Sv
Year
e) Precipitation / GMST
%/°C
Year
f) September Arctic SIA
Million km2
Year

Figure 3.

N.Europe

JJA precipitation timeseries for N.Europe

%

GWL (°C)

Year

Range of trends: -1.62 to 1.01 %/decade

Range of trends: 0.91 to 2.17 %/century

Mediterranean

JJA precipitation timeseries for Mediterranean

%

GWL (°C)

Year

Range of trends: -5.44 to -1.61 %/decade

Range of trends: 0.59 to 1.74 %/century

Jet latitude

Atlantic jet latitude

Lat °N

GWL (°C)

Year

Range of trends: 0.03 to 0.23 °N/decade

Range of trends: -0.06 to 0.08 °N/century

ssp370 parent transient run

hist 2014

2020 SSP370

2025 SSP370

2025 SSP245

2030 SSP119

2040 SSP370

Figure 4.

JJA trends divided by trend in GMST (500/85 years respectively)

Ensemble mean fix. conc. trends

Ensemble mean transient trends

Fix. conc. minus transient trends

Temperature

Sea level pressure

U winds 850hPa

Precipitation

Surf. specific humidity

K/K

2.0
1.5
1.0
0.5
0.0
−0.5
−1.0
−1.5
−2.0

hPa/K

1.00
0.75
0.50
0.25
0.00
−0.25
−0.50
−0.75
−1.00

m*s-1/K

1.00
0.75
0.50
0.25
0.00
−0.25
−0.50
−0.75
−1.00

mm*day-1/K

1.00
0.75
0.50
0.25
0.00
−0.25
−0.50
−0.75
−1.00

g*kg-1/K

1.00
0.75
0.50
0.25
0.00
−0.25
−0.50
−0.75
−1.00